Perspective: AIChE 2010 Alpha Chi Sigma Award Winner

Mechanics of Drying Colloidal Dispersions: Fluid/Solid Transitions, Skinning, Crystallization, Cracking, and Peeling

William B. Russel*
Dept. of Chemical and Biological Engineering, Princeton University, Princeton NJ 08544

DOI 10.1002/aic.12651
Published online May 2, 2011 in Wiley Online Library (wileyonlinelibrary.com).

Keywords: colloids, film formation, drying, latex, cracking

Introduction

The process of drying colloidal dispersions by evaporating the liquid to create particulate solids, porous coatings, or continuous films is common to a range of important technologies, e.g., forming polymer coatings from latex dispersions,[1,2] casting magnetic tapes,[3] depositing highly porous coatings on ink jet papers,[4] forming sol–gel glass,[5] adding antireflection coatings to eyeglass lenses,[6] encapsulating vitamins in beads,[7] fabricating photonic crystals from silica sols,[8] spray depositing thin film oxide fuel cells,[9] and manufacturing photographic film.[10] The objective varies but is generally to create a layer of specified thickness and controlled porosity with permeability, strength, optical, or other physical properties appropriate for the application. The particles often are polymer latices or inorganic oxides, e.g., silica, alumina, or zirconia, and the fluid is normally water, but occasionally is a low-molecular-weight organic. Processing of such films raises a number of interesting and difficult issues because of the conflicting constraints and performance properties imposed by the applications.

The technology advanced considerably for several decades through enlightened and innovative industrial research until a variety of mechanisms, such as Gordon Conferences, university-industry consortia like IPRIME at Minnesota, the International Polymer Colloids Group, the division of Colloid and Surface Chemistry in the American Chemical Society, the UK Polymer Colloid Forum, and European Commission projects that encourage industry-university collaboration, ignited academic interest. This brought into the field powerful, and expensive, modern experimental techniques, as well as theorists having expertise with computational and analytical tools capable of handling multiphase and time-dependent flows. This perspective seeks to provide a glimpse into developments of the past couple of decades that address the process of forming solid materials from fluid dispersions from the initial evaporation of the liquid through the formation of the final film.

As the liquid, assumed hereafter to be water, evaporates the concentration of particles increases but the dispersion remains a fluid until a gelation, freezing, or glass transition is encountered. If the process is slow enough, that is the rate of evaporation relative to diffusion of particles across the liquid layer is sufficiently small, and the interparticle attractions are not abnormally strong, dispersions will eventually reach a random or ordered close packing.[11] Further evaporation deforms the menisci between particles at the air–water interface, generating a negative capillary pressure that puts the dispersion in compression in the direction of evaporation and tension in the transverse directions. This translates into an interparticle force of order $a\gamma$ that easily overcomes any interparticle repulsion of order kT/a, since $a^2\gamma/kT \sim 10^5$ for $a \sim 100$ nm and ~ 10 even for $a \sim 1$ nm; where a = particle radius, kT = thermal energy, and γ = air–water surface tension. Close packing results in sufficient direct contacts between neighbors, e.g., 6 for random packing[12] and 12 for perfect hexagonal order, to immobilize the particles and create a colloidal solid. Shorter range attractions can sustain solids at somewhat lower volume fractions.[13]

As noted by Keddie and Routh,[14] scientific study of the process of latex film formation, a major component of the field, only began in the late 1980s. Experimental studies brought an increasing number of modern tools to bear on the structure of the drying film. Now the temperature gradient bar that monitors film formation and the cantilever that detects stresses have been complemented with cryogenic scanning electron microscopy, environmental scanning electron microscopy, small angle neutron and X-ray scattering, confocal microscopy, NMR profiling with ''gradient at right angles to the field'', scanning probe techniques, ultrasonic profiling, and a myriad of others. These techniques, coupled with classical theory, have elucidated both convective and

*This article resulted from an invitation to Professor Bill Russel to contribute a Perspective, based on his scholarly work that was recognized by AIChE's 2010 Alpha Chi Sigma Award for Chemical Engineering Research.

Correspondence concerning this article should be addressed to W. B. Russel at wbrussel@princeton.edu.

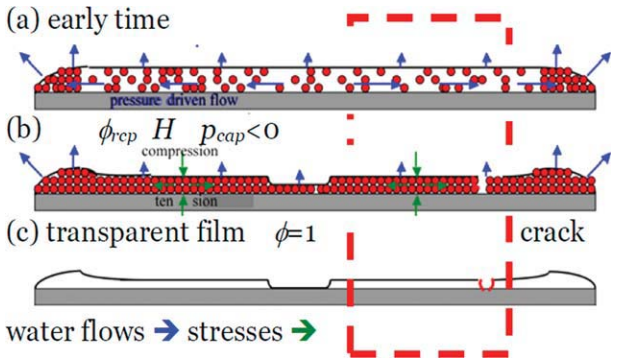

Figure 1. Stages of film formation illustrating (a) packing fronts propagating in from edges, (b) nonuniformity in thickness of close-packed layer, and (c) transparent but cracked final film.

surface tension driven flows while the dispersion remains fluid (Figure 1a). This stage of the process controls the uniformity or nonuniformity of the thickness of the final film (Figure 1b), and can be manipulated to create spatial patterns in the plane or structure in the depth of the film. The subsequent d'Arcy flow and particle deformation after the particles become close packed determine the porosity and the extent of cracking in the final film (Figure 1c).

Effects of convective flows during evaporation

Convection is inevitable during drying and takes several forms, e.g., laterally in the plane of the film due to capillary pressure gradients and toward the air–water interface due to the evaporation, and has several consequences, such as packing fronts that propagate horizontally and vertically; growth of colloidal crystals during slow evaporation; and segregation of binary mixtures to create spatial patterns.

The first widespread attention to surface tension flows during drying was generated by Witten and coworkers,[15] who observed so-called "coffee rings" after the evaporation of a pool of water. They identified nonuniform evaporation and capillary flow as responsible for deposition of nonvolatile components at the periphery. Subsequent analysis by Routh and Russel[16] for concentrated dispersions predicted nonuniformities in the film thickness by coupling nonuniform evaporation due to thinner boundary layers at the edges with capillary pressure gradients that drive lateral flows in the fluid dispersion and d'Arcy flows through the close-packed regions (Figure 1). One important feature of the process is the "open time" before the edge of the film dries. This happens when the capillary pressure reaches the maximum sustainable value, $-5.3\gamma/a$,[17] and the air–water interface recedes into the packing, leaving a dry edge that may not blend with a subsequent application to extend the film, as in painting.

If the close-packed particles deform quickly enough by viscous flow, the voids close completely as the last water evaporates, leaving a transparent film. With higher viscosities or faster evaporation, the air–water interface may recede into the packing, leaving a porous film. With more elastic particles cracks can open to release tension in the plane of the film caused by the capillary pressure. Since the lateral dimensions are generally much greater than the thickness, convection normally dominates in the plane, while diffusion maintains uniformity in the normal direction. In some situations, although, evaporation is rapid relative to diffusion in the normal direction as well, producing close packing first at the air-dispersion interface. That poses the possibility of pores closing at the interface and creating an impervious "skin".

Theories describing these phenomena have been extended and tested by elegant experiments employing NMR profiling.[18] Keddie and coworkers applied the earlier analysis to demonstrate the dependence of the dimensionless "open time", Et_o/H, for a circular film of radius R, and thickness, H, on (1) the characteristic capillary pressure, γ/a, scaled by the nominal pressure drop for d'Arcy flow, $\mu EL^2/kH$, and (2) the ratio of the radius to the capillary length, R/L, where E[m/s] = rate of evaporation, η = dispersion viscosity, μ = fluid viscosity, and k = permeability of packing. The capillary length, $L = H(\gamma/3\eta E)^{1/4}$, reflects the balance between surface tension and viscous stresses within the fluid dispersion. Figure 2 demonstrates the dramatic increase in open time with either the normalized capillary pressure or the R/L.

The distribution of water both laterally and vertically was probed in another series of experiments by Keddie and colleagues.[19] At $Pe = HE/D_0 = 0.2$ (with D_0 = Stokes–Einstein diffusivity of particles) the volume fraction was homogeneous as expected, but for $Pe > 1$ vertical gradients appeared and steepened with increasing Peclet number. At the higher Pe a density gradient emerged at the air–water interface, about half way through the drying time, and evolved into a close-packed layer with $\phi \sim 0.6$ at the air–water interface about $^3/_4$ of the way through.[20] That close-packed layer eventually extended although the full thickness and narrowed as the remaining water gradually disappeared. Under these conditions, latices above their glass transition temperature T_g may deform into an impervious skin that retards further evaporation.[21] A recent article characterizes the process more quantitatively.[22]

Keddie[1] noted in his extensive 1997 review of the field that, "Surfactants are nearly always present in a latex and

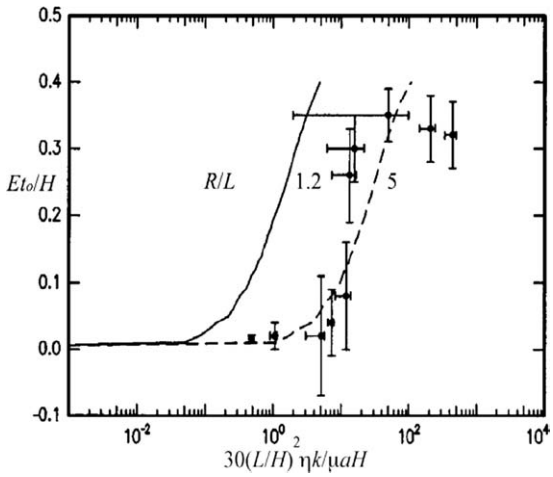

Figure 2. Open time as function of capillary length [$L/H = (\gamma/3\eta E)^{1/4}$], and ratio of viscous to d'Arcy flow (with permission from Salamanca et al.[18]).

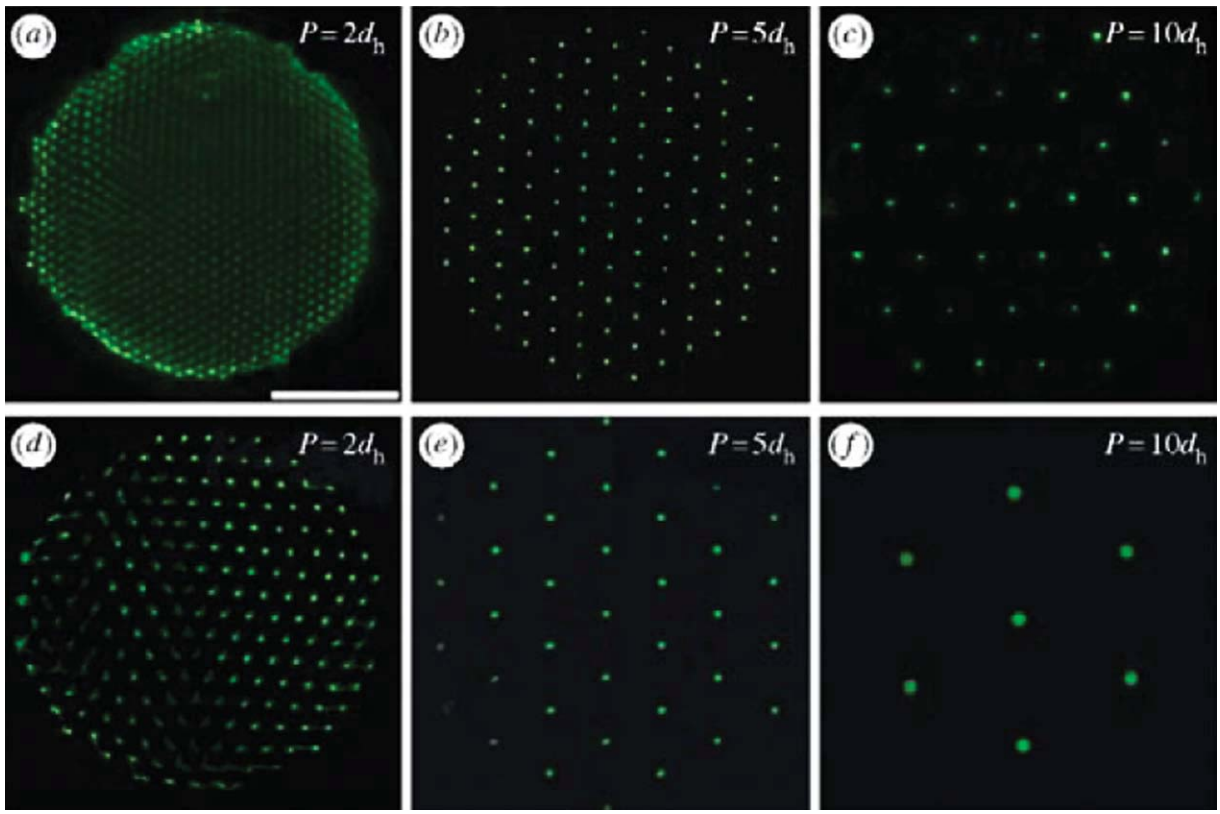

Figure 3. Images illuminating fluorescent nanoparticles of binary films dried under masks with gaps of 250 μm (*a–c*) or 500 μm (*d–f*) and center-to-center distance between holes of 2, 5 or 10 times the gap (with permission from Harris et al.[31]).

are known to affect several aspects of film formation''. Their surface activity promotes partitioning onto both the particle-water and the air–water interfaces in equilibrium with the concentration in the water. Local changes due to fluid convection in the balance between the interfacial area and the fluid volume alter that equilibrium, thereby generating concentration gradients that effect colloidal stability and capillary pressure locally. Spectroscopic measurements have characterized gradients normal to the interface and the effects of surfactant content and type.[23] During drying, while the film is still fluid, a linear stability analysis revealed unstable modes with two distinctly different wavelengths, one at the millimeter scale and the other at microns.[24] The dynamics are driven by evaporation coupled with desorption of surfactant from the air–water interface or the particles. The authors confirmed the phenomena via direct visualization and atomic force microscopy, including the dependence on volume fraction, surfactant concentration, and adsorption strength and the insensitivity to evaporation rate. The short wavelength instability produces striations in the final film, while the longer wavelengths evolve into surfactant-rich islands.

The ability to generate close packing of monodisperse colloids at a controlled rate has stimulated several creative initiatives to form specialized materials. While one-dimensional (1-D) sedimentation of dilute dispersions does form colloidal crystals, the kinematics lead to polycrystalline, rather than single crystal, sediments.[25] Slow sedimentation onto an appropriately patterned substrate can yield a single face-centered-cubic crystal, but stacking faults eventually appear as the crystalline layer grows.[26] For a more practical approach Colvin and coworkers[27] turned to directional evaporation and succeeded in producing single crystal multilayers, but here too stacking faults and cracks eventually appeared. This remains an active field because of the efforts to create optical band gap materials.[28]

Another strategy to create structured films exploits the differential responses of large and small particles to convection during the drying process. The simplest approach depends on evaporation to bring the larger particles into close packing, first at the air–water interface and then throughout the layer.[29,30] Then the interstitial flows convect the smaller particles toward the free surface faster than diffusion can disperse them, creating a vertically segregated film. Deformation of the larger particles closes the voids and quenches this inhomogeneous distribution.

Lewis and coworkers took the next step by imposing a patterned mask, which localizes the evaporation laterally. Once the larger particles reach close packing, the localized evaporation convects particles small enough ($<1/8$ the diameter of the larger ones) to pass through the remaining pores into a periodic pattern conforming to the mask. Figure 3[31,32] demonstrates the final result for two different gaps between the film and the mask and three different spacings for the holes. Resolution is fine except for the smallest spacing and gap.

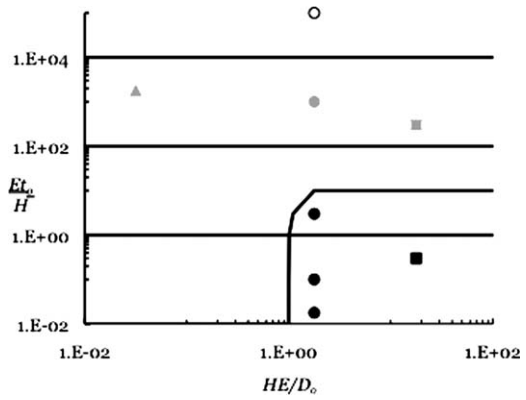

Figure 4. Process map distinguishing among dry and wet sintering and capillary compression, as well as skinning, in terms of the ratio of time scales for viscous flow *to* $=\eta a/\gamma$wa, evaporation H/E, and diffusion H^2/Do.

Symbols indicate experiments conforming to skinning (black), capillary compression followed by dry sintering (gray), and dry sintering (open). (Redrawn with permission from Routh and Russel[41])

Film formation

In many applications the objective is to form an impervious or controllably permeable coating. This requires viscous deformation to eliminate or shrink pores between close-packed polymer spheres at temperatures in the vicinity of the glass temperature. Qualitative understanding has evolved since the invention of monodisperse polymer latices in the 1950s, which spawned the latex paint technology. In the 1990s quantitative measurements began to appear in the literature from both industrial[11] and academic laboratories and eventually quantitative theories followed as described by Routh and Keddie.[14] Although wet and dry sintering, driven by polymer-water and polymer-air interfacial energies, respectively, can close the pores and form a uniform film, the dominant driving force is usually a negative capillary pressure due to inward deflection of menisci at the air–water interfaces between particles. That puts the packing in compression in the normal direction and in tension laterally. Clever use of a taut membrane as the substrate allowed Johannsmann and coworkers[33–35] to translate deformation of the membrane into a clear demonstration of the tensile stresses acting on the film.

Our recent theory,[36] describing the mechanics of this process, starts with Hertizian contact mechanics,[37] augmented by a viscous analogue,[38] that relates the force $\boldsymbol{F}$, between two spheres in contact at orientation $\boldsymbol{n}$, to the deformation ϵ and yields

$$\boldsymbol{F} + 2.74\pi a\gamma_{pa/w}\boldsymbol{n} = -\frac{16}{3}a^2\frac{G}{2(1-v)} \int_{-\infty}^{t} exp((t'-t)/\tau)\frac{d}{dt'}(-\boldsymbol{n}\cdot\boldsymbol{\varepsilon}\cdot\boldsymbol{n})^{3/2}\boldsymbol{n}\,dt' \quad (1)$$

with the characteristic time scale $\tau = 2\eta(1-v)/G$, where η, G, and v are the viscosity, shear modulus, and Poisson ratio of the polymer, respectively. Thus, one can discriminate between fast evaporation ($E\tau$/H>1), which triggers an elastic response, and slow evaporation ($E\tau$/H<1) for which the response is viscous. Volume averaging over doublets of all orientations *a la* Batchelor[39] yields a nonlinear time-dependent stress–strain relationship, which for 1-D deformation takes the following form

$$\sigma_{zz} = -\left(p_{cap} - 0.69\frac{\phi N\gamma_{a/wp}}{a}\right) - \frac{2}{3}\bar{G} \int_{-\infty}^{t} \exp((t'-t)/\tau)\frac{d\varepsilon^{3/2}}{dt'}dt' = 0 \quad (2)$$

where $\overline{G} = N\phi G/(1-v)$, N = number of neighbors in contact, and ϕ = packing fraction. Note that the free surface imposes the zero normal stress.

Integrating Eq. 2 determines the evolution of the density, setting the time required to close the pores, when $\epsilon = 1 - \phi = 0.36$, and identifying whether capillary compression, wet sintering (γ_{wp} = water-polymer interfacial tension), or dry sintering (γ_{ap} = air-polymer interfacial tension) controls the process. When evaporation is rapid relative to diffusion and the particles deform easily, an impermeable skin can form at the air–water interface sealing off further evaporation. Figure 4[40,41] maps the various regimes in terms of $Ea\eta/H\gamma$, the rate of evaporation relative to viscous deformation of the packing driven by capillary pressure, and the Peclet number $Pe = HE/D_o$, for convection and diffusion normal to the interface. Note that wet sintering controls film formation, when evaporation is slow relative to viscous deformation, while capillary compression provides the driving force at intermediate evaporation rates. Only dry sintering can complete the process for very rapid evaporation, after the air–water interface recedes into the film when the negative capillary pressure reaches the maximum of $5.3\gamma/a$. Skinning, i.e., formation of an impermeable layer at the air–water interface, occurs for very rapid deformation and slow diffusion, Pe>1 (lower right in the diagram), in accord with the experiments noted previously. For polymer latices the controlling process parameter is the polymer viscosity, which varies exponentially with the temperature relative to the glass transition of the polymer. Then the time for void closure for wet or dry sintering increases exponentially with $T_g - T$.[40] For $T_g \sim T$ capillary compression closes the pores as the last water evaporates, at $t = (1-\phi_o)H/E$.

The groups of Scriven at Minnesota[42,43] and Lewis at Illinois[44] first quantified the tensile stress associated with drying films of a few square centimeters with the classic cantilever technique. Typically, for latices that deform viscously in response to capillary pressure, the stress increases as $t^{3/2}$ after the dispersion becomes close packed, reaching a maximum that is proportional to $\eta\dot{E}/H$ as the last pores close (Figure 5).[45] Note that the stress (capillary pressure) remains well below the maximum of $5.3\gamma/a$ in these experiments.

Cracking and peeling in colloidal films

When particles do not deform viscously, the capillary pressure produces elastic deformation that stores energy in the packing and, therefore, is capable of generating cracks in the films.[46] To understand this we turn to the analogous treatment for thin elastic films,[47,48] which invokes the Griffiths criterion that the elastic energy recovered by opening a

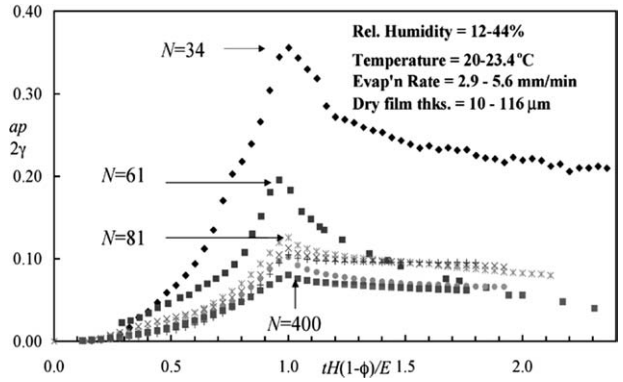

Figure 5. Tensile stress in films of aqueous acrylic latices as a function of time over a small range of temperatures, a modest range of evaporation rates, and a 10-fold variation in film thickness, demonstrating that pores close at $\sigma_{max} \sim \eta E/H$ as evaporation is complete at $t \sim H(1-\phi)/E$ (with permission from Tirumkudulu and Russel[45]).

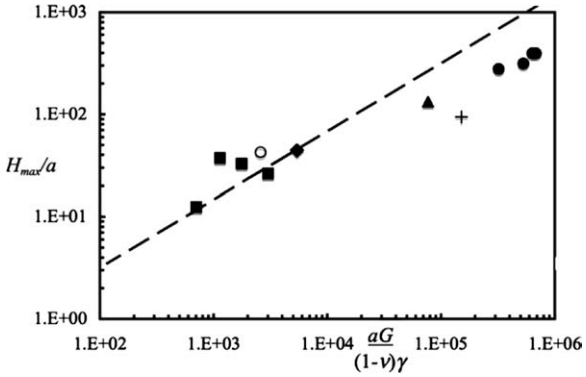

Figure 6. Film thickness below which cracking is energetically unfavorable according to theory (- - - -) and dispersions of polymer latices (■), and oxides (●) show no cracks (redrawn with permission from Singh and Tirumkudulu[50]).

crack must match or exceed the surface energy expended. For saturated films the dominant surface energy is that of the air–water interface of the crack faces, while the elastic energy is recovered during the relaxation of the particles compressed at point contacts in the close packing.

An estimate of the elastic recovery upon the opening of an infinite crack can be derived by linearizing the general nonlinear stress–strain relation about the 1-D compression and then either solving the resulting set of partial differential equations numerically or by integrating in the normal direction *a la* lubrication and then solving the resulting ordinary differential equation analytically.[49] Setting the total elastic energy recovered equal to the energy of the new air–water surface determines the minimum capillary pressure p_{cap}^{crack} to open a crack as[36]

$$-\frac{Hp_{cap}^{crack}}{\gamma} \cong 1.3\left(\frac{\phi NGH}{2(1-\nu)\gamma}\right)^{2/5} + 2.9\frac{\gamma}{\phi N\eta\dot{E}}\frac{\phi NGH}{2(1-\nu)\gamma}. \quad (3)$$

Note that viscous deformation increases the capillary pressure necessary for cracking, as does reducing the film thickness. Experiments suggest this to be a reasonable approximation. For example, measurements of H_{min}, the film thickness below which the air–water interface recedes into the packing without causing cracking,[50] follow the theory (- - -) reasonably well for both polymer latices (lower left), and inorganic oxides (upper right) (Figure 6).

Direct measurements of the capillary pressure at the onset of cracking for latices demonstrate independence of the particle size as expected by theory for high T_g polymer latices (Figure 7), but consistently lie above the prediction. Furthermore, data for the latices do not correlate with that for inorganic oxides. Subsequent introduction of microscopic flaws (grain boundaries in crystalline packings) or macroscopic notches in the O-ring bounding the cell (not shown) brought the data closer to the prediction.[51] This suggests that flaws or imperfections are necessary to initiate cracking in colloidal packings. In retrospect, this should not have been a surprise, as their importance in brittle solids is well known.[52]

Singh et al.[13] adapted the theory to alumina dispersions at a range of pHs encompassing both fully stable and highly flocculated conditions. This required measuring or estimating from correlations in the literature the packing fractions (from $\phi \sim 0.15$ near the isoelectric point to ~ 0.70 for stable dispersions), the number of contacting neighbors ($N = 1$-7), and the maximum capillary pressure ($3\gamma\phi\cos\theta/a(1-\phi)$ with θ the air–water-polymer contact angle). The corresponding critical cracking thickness varied dramatically from ~ 50 μm at stable conditions to ~ 300 μm near the isoelectric point, reflecting the combination of a lower maximum capillary pressure and weaker elastic response for the less dense packing. The critical stress for the onset of cracking correlated well with $N\phi/H^2$ to the $^1/_3$ to $^2/_5$ power, indicating a more deformable packing that cracks easier.

Another popular geometry for studying drying of dispersions consists of a rectangular capillary open to evaporation at one end (Figure 8a).[53] This produces a well-defined packing front that propagates into the capillary and defines a uniform gradient in capillary pressure from a minimum at the

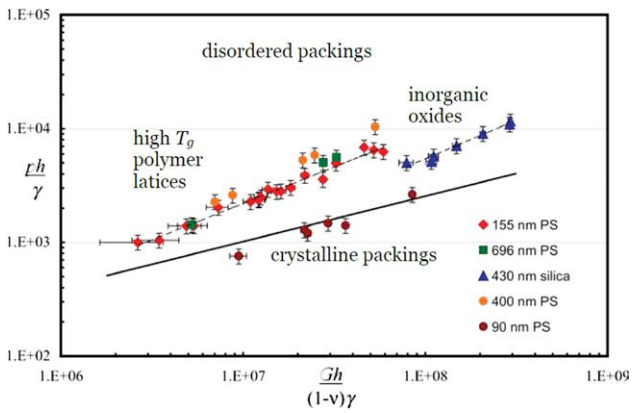

Figure 7. Capillary pressure at the onset of cracking for disordered packings of high *Tg* polystyrene latices and inorganic oxides and crystalline packings of deionized monodisperse latices (redrawn with permission from Lawn[51]).

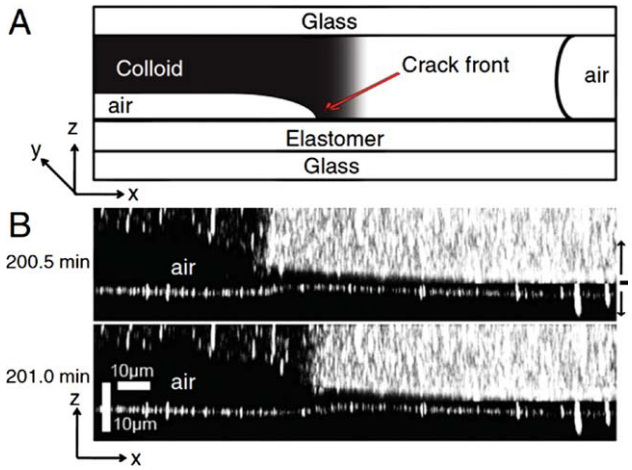

Figure 8. (a) Schematic cross section of rectangular capillary illustrating open end on left, shading to indicate colloid density, and delamination from surface at the bottom, and (b) microscopic images 30 s apart of the cross section with PDMS layer at the bottom showing the advancement of the delamination front (with permission from Xu et al.[54]).

open end to zero at the packing front. With nanoparticles the capillary pressure at the free surface quickly reaches the limit noted earlier, allowing the air–water interface to recede into the capillary and introducing an additional mass-transfer resistance in the form of Knudsen diffusion, which slows evaporation. Microscopic tracking of cracks revealed "intriguing intermittent motion originating from the deformation of arrested crack tips and aging of the elastic network".

A recent study in the same geometry, but with a novel means for sensing stresses in the colloidal packing,[54] detected failure or delamination between the colloidal packing and the surface of the capillary. This "interface crack" corresponds to peeling for a free-standing thin film (Figure 8b). The authors tracked the stress and strain fields, deducing decay as the inverse square root of distance from the crack tip, consistent with cracking in elastic films. Our subsequent analysis[55] based on the Hertzian mechanics described earlier, confirms recovery of elastic energy as the mechanism for debonding, which allows some relaxation of the axial compression driven by the pressure gradient. The theory also predicts the lag of the delamination front behind the packing front in qualitative agreement with the observations.

Cracking also occurs during directional drying in thin films open to the atmosphere.[46] As noted earlier, the mass-transfer boundary layer in the air is thinner at the edges, allowing more rapid evaporation that initiates packing and cracking fronts that propagate from the edges into the interior. In such a situation, a recent study by Goehring et al.[56] with charged polymer latices visualize several fronts. First is a somewhat diffuse jump in concentration from the original fluid dispersion to an ordered and iridescent, but not close-packed, solid. Next is a sharp transition to ordered close packing with particles in mechanical contact. This transition from loose to close packing signals flocculation, with particles pushed over the repulsive electrostatic barrier into contact by the increasing capillary pressure. This was verified by flooding the film with water and observing that the loosely packed region redispersed, whereas the close-packed particles remained a coherent solid. To emphasis this further, parallel cracks followed the solidification front, albeit intermittently, consistent with the need for relaxation of elastically deformed particles in contact to recover elastic energy. None of the fronts propagated at a steady velocity with the cracks being most intermittent as observed earlier by others.[53]

In Closing

Both understanding and implementation of drying processes have advanced considerably in the past 2 decades, including a number of facets not addressed here, such as binary mixtures of soft and hard particles[57] and subtle dynamics as the air–water interface recedes into the colloidal packing.[58] The focus of this perspective has been the complex phenomena that emerge as the process of gas-phase controlled evaporation drives fluid flow in a thin film. Loss of fluid moves the initially fluid dispersion across one or more phase boundaries into a dense solid that a rising capillary pressure then deforms either elastically or viscously. The former often leads to cracking and peeling, while the latter produces a pore-free solid. A number of important technologies noted in the introduction exploit the process and several other novel applications have been suggested more recently.

Acknowledgments

The author's interest in this field was stimulated by discussions over a decade or more with Peter R. Sperry at Rohm & Haas and was advanced through collaborations with Alexander F. Routh, now at Cambridge University; Mahesh S. Tirumkudulu, now at IIT Bombay; Weining Man, now at San Francisco State University; and Ning Wu, now at the Colorado School of Mines. Meetings of the "Cracking Club", including Richard Buscall of ICI and Eric Dufresne of Yale, provided periodic stimuli. Funding from the National Science Foundation and the Petroleum Research Fund supported the work.

Literature Cited

1. Keddie JL. Film formation of latex. *Mater Sci Eng*. 1997;21(3).
2. Winnik MA. *The formation and properties of latex films*. In: Lovell PA, El-Aasser MS, eds. *Emulsion Polymerization and Emulsion Polymers*. Chichester, U.K: John Wiley & Sons; 1997; 467–518.
3. Martinez CJ, Lewis JA. Rheological, structural, and stress evolution of aqueous Al2O3 latex tape-cast layers. *J Am Ceram Soc*. 2002;85(10):2409–2416.
4. Wedin P, Martinez CJ, Lewis JA, Daicic J, Bergstrom L. Stress development during drying of calcium carbonate suspensions containing cabooxymethylcellulose and latex particles. *J Colloid Interface Sci*. 2004;272:1–9.
5. Brinker JC, Scherer GW. *Sol-Gel Science: The Physics and Chemistry of Sol-Gel Processing*. Elsevier; 1989.
6. Amalvy JI, Percy MV, Armes SP. Synthesis and characterization of novel film-forming vinyl polymer/silica colloidal nanocomposites. *Langmuir*. 2001;17:4770–4778.

7. Clegg JB. Process of preparing vitamin-containing gelled aqueous colloid beads. US Patent 3,445,563. 1969.
8. Saunders AE, Shah PS, Sigman MB, Hanrath T, Hwang HS, Lim KG, Johnston KP, Korgel BA. Inverse opal nanocrystal superlattice films. *Nano Lett*. 2004;4(10): 1943–1948.
9. Pham A.-Q.; Lee TH, Glass RS. In: Colloidal spray deposition technique for the processing of thin film solid oxide fuel cells. 196th Meeting of the Electrochemical Society, Honolulu HI, Oct. 17, 1999.
10. Huang CC. Asymptotic drying of gelatic in photographic film. *J Math Anal Appl*. 1994;187(2):663–675.
11. Sperry PR, Snyder BS, O'Dowd ML, Lesko PM. Role of water in particle deformation and compaction in latex film formation. *Langmuir*. 1994;10(8):2619–2628.
12. Donev A, Cisse I, Sachs D, Variano E, Stillinger FH, Connelly R, Torquato S, Chaikin PM. Improving the density of jammed disordered packings using ellipsoids. *Science*. 2004;303(5660):990–993.
13. Singh KB, Bhosale LR, Tirumkudulu MS. Cracking in drying colloidal films of flocculated dispersions. *Langmuir*. 2009;25(8):4284–87.
14. Keddie JL, Routh AF. *Fundamentals of Latex Film Formation*. The Netherlands: Springer; 2010.
15. Deegan RD, Bakajin O, Dupont TF, Huber G, Nagel SR, Witten TA. Capillary flow as the cause of ring stains from dried liquid drops. *Nature*. 1997;389:827–9.
16. Routh AF, Russel WB. Horizontal drying fronts during solvent evaporation from latex films. *AIChE J*. 2002; 48(4):917–918.
17. Mason G, Mellor DW. Simulation of drainage and imbibitions in a random packing of equal spheres. *J Colloid Interface Sci*. 1995;176: 214–255.
18. Salamanca JM, Ciampi E, Faux DA, Glover PM, McDonald PJ, Routh AF, Peters ACIA, Satguru R, Keddie JL. Lateral drying in thick films of waterborne colloidal particles *Langmuir*. 2001;17(11): 3202–3207.
19. Gorce J-P, Bovey D, McDonald PJ, Palasz P, Taylor D, Keddie JL. Vertical water distribution during the drying of polymer films cast from aqueous emulsions. *Euro Phys J E*. 2002;8:421–429.
20. König AM, Weerakkody TG, Keddie JL, Johannsmann D. Heterogeneous drying of colloidal polymer films: dependence on added salt. *Langmuir*. 2008;24:7580–7589.
21. Mallegol J, Bennett G, McDonald PJ, Keddie JL, Dupont O. The skin development during the film formation of waterborne acrylic pressure-sensitive adhesives containing tackifying resin. *J Adhes*. 2006;82:217–238.
22. Ekanayake P, McDonald PJ, Keddie JL. An experimental test of the scaling prediction for the spatial distribution of water during the drying of colloidal films. *Euro Phys J*. 2009;166:21–27.
23. Tzitzinou A, Jenneson PM, Clough AS, Keddie JL, Lu JR, Zhdan P, Treacher KE, Satguru R. Surfactant concentration and morphology at the surfaces of acrylic latex films. *Prog Org Coat*. 1999;35:89–99.
24. Gundabala VR, Lei C-H, Ouzineb K, Dupont O, Keddie JL, Routh AF. Lateral surface nonuniformities in drying latex films. *AIChE J*. 2008;54(12):3092–3105.
25. Davis KE, Russel WB, Glantschnig WJ. Disorder-to-order transition in settling suspensions of colloidal silica - x-ray measurements. *Science*. 1989;245(4917):507–510.
26. Blaaderen A v, Ruel R, Wiltzius PA. Template-directed colloidal drystallization. *Science*. 1997;385(6614):321–324.
27. Jiang P, Bertone JF, Hwang KS, Colvin VL. Single-crystal colloidal multilayers of controlled thickness. *Chem Mater*. 1999;11(8):2132–2140.
28. Petukhov AV, Dolbnya IP, Aarts DGAL, Vroege GJ. Destruction of long-range order recorded with in situ small-angle x-ray diffraction in drying colloidal crystals. *Phys Rev E*. 2004;69:031405.
29. Luo H, Cardinal CM, Scriven LE, Francis LF. Ceramic nanoparticle/monodisperse latex coatings. *Langmuir*. 2008; 24(10):5552–5561.
30. Nikiforow I, Adams J, Konig AM, Langhoff A, Pohl K, Turshatov A, Johannsmann D. Self-stratification during film formation from latex blends driven by differences in collective diffusivity. *Langmuir*. 2010;26(16):13162–13167.
31. Harris DJ, Conrad JC, Lewis JA. Evaporative lithographic patterning of binary colloidal films. *Philos Trans R. Soc London, Ser A*. 2009;367:5157–5165.
32. Harris DJ, Hu H, Conrad JC, Lewis JA. Patterning colloidal films via evaporative lithography. *Phys Rev Lett*. 2007;98:148301.
33. Ehe K vd, Johannsmann D. Maps of the stress distributions in drying latex films. *Rev Sci Instrum*. 2007; 78(11):113904.
34. Konig AM, Bourgeat-Lami E, Mellon V, Ehe K vd, Routh AF, Johannsmann, D. Dilational lateral stress in drying latex films. *Langmuir*. 2010;26(6):3815–3820.
35. Konig AM, Johannsmann D. Stress fluctuations in drying polymer dispersions. *Langmuir*. 2010;26(12):9437–9441.
36. Russel WB, Wu N, Man M. A generalized Hertzian model for the deformation and cracking of colloidal packings saturated with liquid. *Langmuir*. 2008;24:1721–30.
37. Johnson K L. *Contact Mechanics*. Cambridge: Cambridge University Press; 1985.
38. Matthews JR. Indentation hardness and hot pressing. *Acta Metall*. 1980;28;311–318.
39. Batchelor GK. The stress system in a suspension of force-free particles. *J Fluid Mech*. 1970;41:545–570.
40. Routh AF, Russel WB. A process model for latex film formation: Limiting regimes for individual driving forces. *Langmuir*. 1999; 15(22):7762–7773.
41. Routh AF, Russel WB. Deformation mechanisms during latex film formation: Experimental evidence. *Ind Eng Chem Res*. 2001;40(20): 4302–08.
42. Lei H, Payne JA, McCormick AV, Francis LF, Gerberlich WW, Scriven LE. Stress development in drying coatings. *J Appl Polym Sci*. 2001;81(4):1000–1013.
43. Lei H, Francis LF, Gerberich WW, Scriven LE. Stress development in drying coatings after solidification. *AIChE J*. 2002;48(3):437–451.
44. Martinez CJ, Lewis JA. Shape evolution and stress development during latex-silica film formation. *Langmuir*. 2002;18(12):4689–4698.
45. Tirumkudulu MS, Russel WB. Role of capillary stresses in film formation. *Langmuir*. 2004;20(7):2947–2961.
46. Tirumkudulu MS, Russel WB. Cracking in drying latex films. *Langmuir* 2005;21:(11):4938–4948.

47. Evans AG, Drory MD, Hu MS. The cracking and decohesion of thin films. *J Mater Res*. 1988;3(5):1043–1049.
48. Beuth JL. Cracking of thin bonded films in residual tension. *Int J Solids Struct*. 1992;29(13):1657–75.
49. Xia XC, Hutchinson JW. Crack patterns in thin films. *J Mech Phys Solids*. 2000;48(6–7):1107–1131.
50. Singh KB, Tirumkudulu MS. Measurement of critical thickness for cracking in colloidal films. *Phys Rev Lett*. 2007;98:218302.
51. Man W, Russel WB. Direct measurements of critical stresses and cracking in thin films of colloid dispersions. *Phys Rev Lett*. 2008; 100(19):198302.
52. Lawn B. *Fracture of Brittle Solids*. 2nd ed. Cambridge: Cambridge University Press; 1993.
53. Dufresne ER, Stark DJ, Greenblatt NA, Cheng JX, Hutchinson JW, Mahadevan L, Weitz DA. Dynamics of fracture in drying suspensions. *Langmuir*. 2006;22(17):71447147.
54. Xu Y, Engl WC, Jerison ER, Wallenstein KJ, Hyland C, Wilen LA, Dufresne E. R. Imaging in-plane and normal stresses near an interface crack using traction force microscopy. *Proc Nat Acad Sci*. 2010;107:(34):14964–14967.
55. Wallenstein KJ, Russel WB. Theory of delamination during drying of confined colloidal suspensions. *Phys Chem Chem Phys*. 2011, accepted.
56. Goehring L, Clegg WJ, Routh AF. Solidification and ordering during directional drying of a colloidal dispersion. *Langmuir*. 2010;26(12): 9269–75.
57. Singh KB, Deoghare G, Tirumkudulu MS. Cracking in soft-hard latex blends: theory and experiment. *Langmuir*. 2009;25(2):751–760.
58. Xu L, Davies S, Schofield AB, Weitz DA. Dynamics of drying in 3D porous media. *Phys Rev Lett*. 2008;101(9): 0954502.